Journal of Physics: Conference Series **2586** (2023) 012014 doi:10.1088/1742-6596/2586/1/012014

Results on light (anti)hypernuclei production with ALICE at the LHC

Esther Bartsch for the ALICE collaboration

Goethe-University Frankfurt, Max-von-Laue-Str. 1, 60438 Frankfurt, Germany

E-mail: esther.bartsch@cern.ch

Abstract. The high collision energies reached at the LHC lead to significant production yields of light (anti)hypernuclei in proton–proton (pp), proton–lead (p–Pb) and, in particular, Pb–Pb collisions. The lightest known hypernucleus is the hypertriton, which is a bound state of a proton, a neutron, and a Λ hyperon. It decays weakly with a decay length of a few centimeters. The excellent tracking and particle identification capabilities of the ALICE detector, exploiting the energy loss measurement of the Time Projection Chamber (TPC) and using the Inner Tracking System (ITS) to distinguish between primary and secondary (decay) vertices, allow for the determination of the hypertriton yield across different collision systems, its lifetime, and its binding energy. The latest hypertriton lifetime measurement in Pb–Pb collisions performed in the 2-body decay channel will be presented. This measurement contributes to the solution of the hypertriton lifetime puzzle. In addition, the hypertriton production in different collision systems and at different energies will be compared to model predictions. Due to its low binding energy, and hence to its large size, the hypertriton is the ideal candidate to distinguish between statistical hadronization and coalescence models. With the precision of the presented yield measurements some variants of the aforementioned models can be excluded.

1. Introduction

In ultrarelativistic heavy-ion collisions at the Large Hadron Collider (LHC), a state of deconfined strongly interacting matter consisting of quarks and gluons, called the quark–gluon plasma (QGP), is created. Afterwards, the QGP expands and cools down, until it reaches the pseudo-critical temperature T_{c}. When the chemical freeze-out temperature T_{ch} is reached the hadron yields are fixed, but there can still be elastic interactions between the particles. After the kinetic freeze-out (characterised by T_{kin}) the momentum spectra of the particles do not change anymore. The abundances of different particle species after hadronization provide information about their production mechanism. Among these particles, light (anti)(hyper)nuclei are of special interest since they are loosely bound objects. Their binding energies are very small compared to the chemical and kinetic freeze-out temperatures and their production mechanism is still not completely understood. There are two classes of models available to describe (hyper)nuclei production: the statistical hadronization model [1, 2] and the coalescence model [3, 4].

In the statistical hadronization or thermal model, the production of (hyper)nuclei happens at the chemical freeze-out in thermal equilibrium with all other hadrons and depends exponentially on the particle mass. In (central) heavy-ion collisions, the system can be described by a grand-canonical ensemble where the free parameters are the baryochemical potential μ_{B}, the volume V, and the temperature T_{ch} at chemical freeze-out. μ_{B} has to be introduced to ensure the average

conservation of particle numbers, as the system exchanges particles. For a certain collision energy, a fit to the measured particle yields can be performed to determine V, T_{ch}, and μ_{B}. However, at LHC energies μ_{B} is close to zero. For small systems, i.e. pp and p–Pb, a canonical approach is used, where the quantum numbers (baryon number B, strangeness S, and isospin I_3) are locally conserved rather than on average. For more details see Ref. [2].

In the coalescence model, (hyper)nuclei are produced roughly at the kinetic freeze-out and the production depends on the wave functions of the nuclear species, which also determine their size. The coalescence probability is calculated from the overlap of the phase-space distributions of (point-like) nucleons and the Wigner density of the nucleus, which is the quantum mechanical equivalent of the phase-space distribution. The nuclei can break apart during the system evolution and be recreated by final state coalescence. In the case of nuclei with three constituents the formation process can proceed either in one step (three-body coalescence) or two consecutive steps (two-body coalescence) [5].

Light (anti)(hyper)nuclei are produced at the LHC in pp, p–Pb, and Pb–Pb collisions. The large high-quality data samples in Pb–Pb collisions at $\sqrt{s_{\mathrm{NN}}} = 5.02$ TeV as well as in pp and p–Pb collisions at several collision energies collected by the ALICE Collaboration provide a unique opportunity to study the production mechanism of these loosely bound objects. Results on the hypertriton ($^3_\Lambda$H) are shown in these proceedings.

The hypertriton is a bound state of a proton, a neutron, and a Λ hyperon. With a mass of about $2.99\,\mathrm{GeV}/c^2$ it is the lightest bound hypernucleus. Recent calculations predict a radius for the hypertriton wave function of $10.79^{+3.04}_{-1.53}$ fm [6]. The large size of the hypertriton and the similar mass to other nuclei with mass number $A = 3$ makes it the ideal candidate to distinguish between statistical hadronization and coalescence models.

The hypertriton decays weakly after a few cm. Possible are two-body decays in ^{3}He and charged pion or triton and neutral pion and three-body decays in deuteron, proton (neutron), and charged (neutral) pion. The present measurements of the hypertriton are focussing on the two-body decay $^3_\Lambda\mathrm{H} \rightarrow {}^3\mathrm{He} + \pi^-$. The hypertriton is reconstructed via its daughter particles, which point to the secondary vertex. The daughter particles are identified in the Time Projection Chamber (TPC) via their specific energy loss $\mathrm{d}E/\mathrm{d}x$ with an excellent resolution of about 6 %. With the identified tracks the decay vertex of the hypertriton is reconstructed. The Inner Tracking System (ITS) can distinguish between primary and secondary vertices with a resolution better than $100\,\mu$m in Pb–Pb collisions.

The hypertriton production in small systems will be presented, allowing to study its production as a function of charged-particle multiplicity. Furthermore, the latest determination of hypertriton properties like binding energy and lifetime by the ALICE Collaboration will be reported.

2. Hypertriton in small systems

The hypertriton was for the first time measured in pp collisions at $\sqrt{s} = 13\,\mathrm{TeV}$ and in p–Pb collisions at $\sqrt{s_{\mathrm{NN}}} = 5.02\,\mathrm{TeV}$ [7]. In pp collisions topological and kinematic selections were used for the signal extraction while in p–Pb collisions a machine learning approach was applied. Figure 1 (left and right) shows the invariant mass peaks of the combined hypertriton and antihypertriton analyses in pp and p–Pb collisions, respectively.

To investigate the production mechanism the hypertriton-over-Λ ratio and the S_3 value, which is a double ratio of $^3_\Lambda$H/^{3}He over Λ/p, can be studied. As mentioned before, the large size of the hypertriton influences strongly its production mechanism. In the statistical hadronization model the object size is not relevant while in the coalescence picture a large suppression of the production in small systems is expected due to the object size.

Figure 2 (left) shows the hypertriton-over-Λ ratio versus multiplicity. The black lines represent the statistical hadronization model [8] for two different correlation volumes

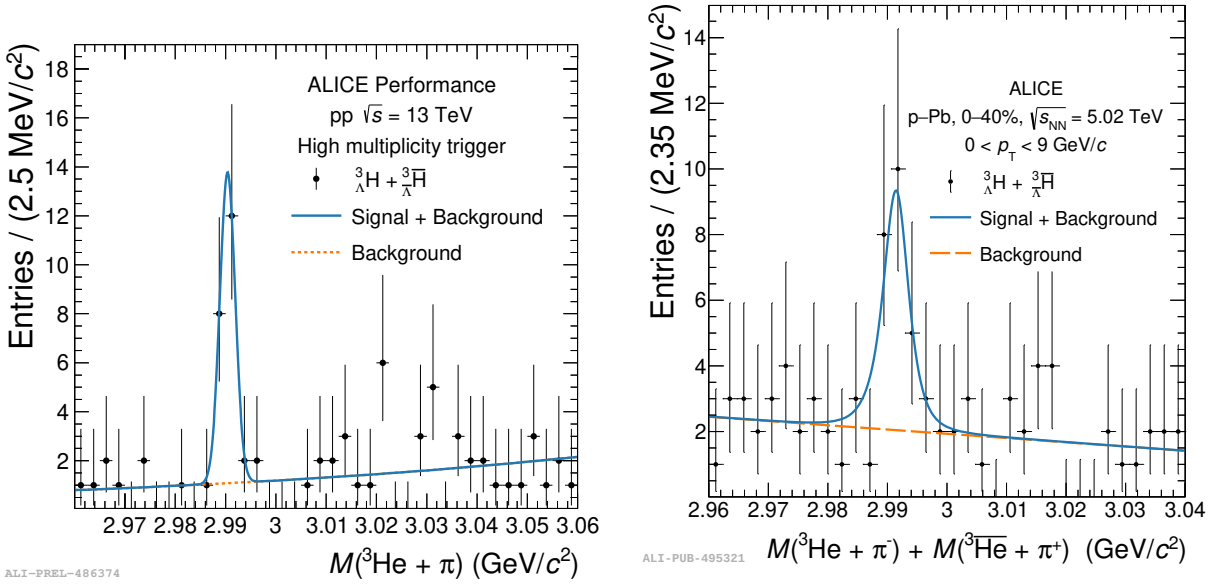

Figure 1. Invariant-mass distribution of the hypertriton in pp collisions at $\sqrt{s} = 13\,\text{TeV}$ (left) and in p–Pb collisions at $\sqrt{s_{\text{NN}}} = 5.02\,\text{TeV}$ (right).

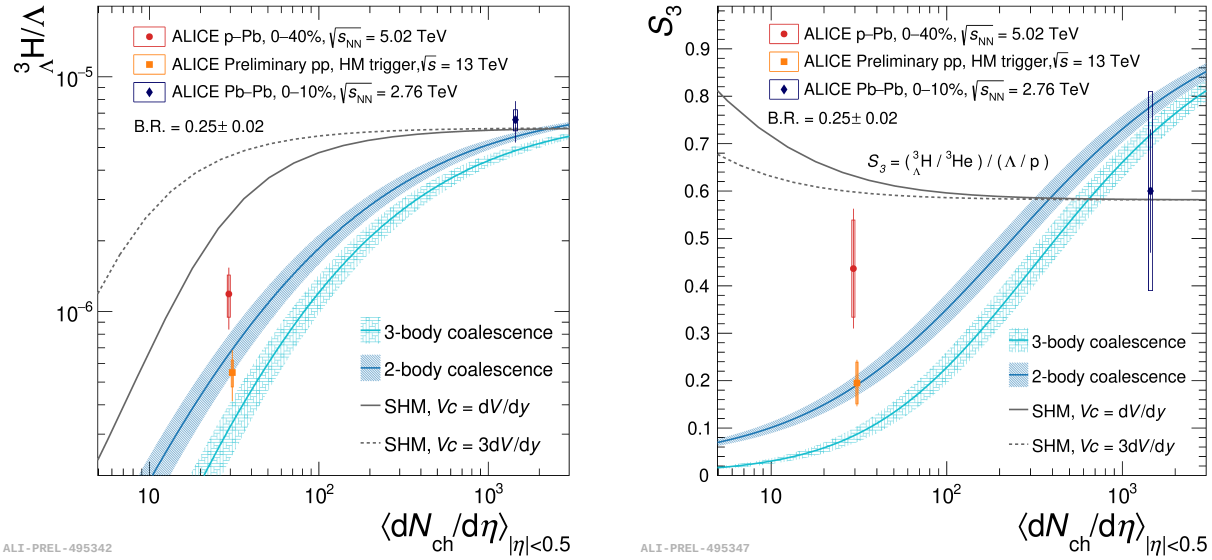

Figure 2. Hypertriton-over-Λ ratio (left) and S_3 value (right) versus multiplicity. The black lines represent the statistical hadronization model [8] for two different correlation volumes, while the blue lines represent the two-body and three-body coalescence [5].

corresponding to one unit (solid) and three units (dashed) of rapidity. The coalescence model [5] is shown as blue lines, while dark blue represents the two-body coalescence and light blue the three-body coalescence. At high multiplicities, i.e. large collision systems, there is nearly no difference between the statistical hadronization and the coalescence model. Whereas at small multiplicities, i.e. small collision systems, a sizeable difference can be observed. The dark blue data point at high multiplicities was measured in Pb–Pb collisions at $\sqrt{s_{\text{NN}}} = 2.76\,\text{TeV}$ [9]. With the new measurements in pp and p–Pb collisions two points at lower multiplicities could be

added (orange and red, respectively). This leads to an exclusion of the statistical hadronization model implementation with the larger correlation volume by more than $6\,\sigma$. Furthermore, the data slightly favour the two-body coalescence but do not exclude the three-body coalescence.

Figure 2 (right) shows the strangeness population factor $S_3=\frac{^3_\Lambda\mathrm{H}/^3\mathrm{He}}{\Lambda/\mathrm{p}}$ versus multiplicity. The S_3 double ratio is supposed to provide information about baryon-strangeness correlations. Furthermore, the penalty factor due to the mass difference and the strangeness production drop out and size effects can be studied. Also here the black lines represent the statistical hadronization model [8] for two different correlation volumes and the dark and light blue lines the two-body and three-body coalescence [5], respectively. At low multiplicities there is a pronounced difference between the models. The two data points at different multiplicities from the pp and p–Pb measurement slightly favour the two-body coalescence without excluding the three-body coalescence.

3. Hypertriton properties

The hypertriton properties were measured in the Pb–Pb data sample at $\sqrt{s_{\mathrm{NN}}} = 5.02\,\mathrm{TeV}$ with unprecedented precision. The signal was extracted using a machine learning approach. Figure 3 shows the invariant mass peak of hypertriton and antihypertriton signals combined.

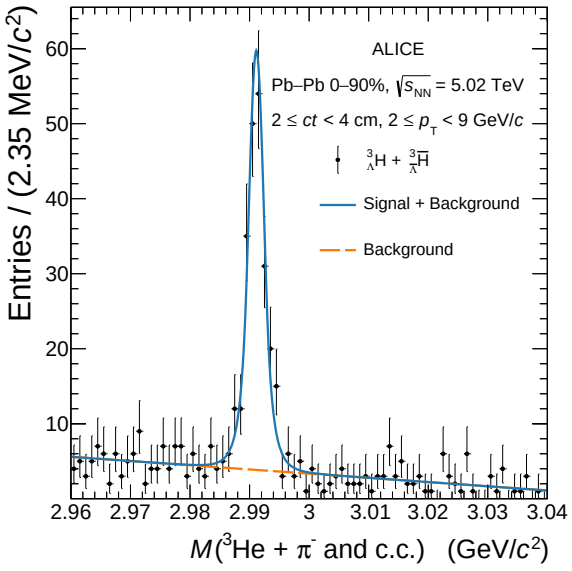

Figure 3. Invariant-mass distribution of the hypertriton in Pb–Pb collisions at $\sqrt{s_{\mathrm{NN}}} = 5.02\,\mathrm{TeV}$ [10].

Figure 4 (left) shows a collection of the hypertriton lifetime measurements obtained by different experiments [10]. The horizontal lines represent the statistical, the boxes the systematic uncertainties. The ALICE data point in red is the most precise measurement so far. It is compatible with the free Λ lifetime, which is shown as vertical black line. This supports a very loosely-bound state. The dashed and dashed-dotted vertical lines depict different theoretical predictions. The ALICE measurement increased the world average lifetime value significantly.

In Fig. 4 (right) a collection of measurements of the Λ separation energy obtained by different experiments is shown [10]. The horizontal lines represent the statistical, the boxes the systematic uncertainties. The ALICE measurement is represented in red. It is the most precise value so far and compatible with the latest theoretical prediction shown as blue band [6].

4. Hypertriton production: baryochemical potential

The hypertriton and antihypertriton yields in Pb–Pb collisions at $\sqrt{s_{\mathrm{NN}}} = 5.02\,\mathrm{TeV}$ were measured in the 0–5 %, 5–10 %, and 30–50 % centrality intervals. The antihypertriton-to-

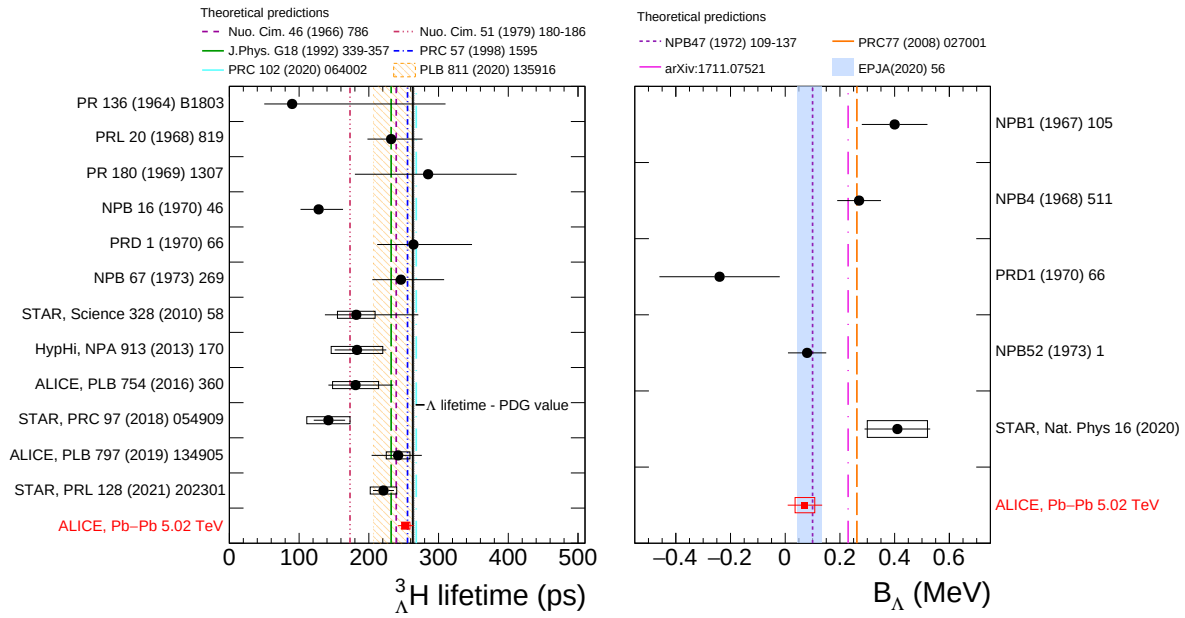

Figure 4. Collection of the hypertriton lifetime (left) and the Λ separation energy (right) obtained by different experiments [10]. The horizontal lines are the statistical, the boxes the systematic uncertainties. The ALICE data points (red) are the most precise measurements to date.

hypertriton ratios are shown in Fig. 5. In all three centrality intervals the ratio is compatible with one.

With the antiparticle-to-particle ratios as input the baryochemical potential μ_B can be determined according to

$$\overline{h}/h = \exp\left[-2\left(B + \frac{S}{3}\right)\frac{\mu_B}{T_{\rm ch}} - 2I_3\frac{\mu_{I_3}}{T_{\rm ch}}\right], \tag{1}$$

where B is the baryon number, S the strangeness, $T_{\rm ch}$ the chemical freeze-out temperature, I_3 the isospin, and μ_{I_3} the isospin chemical potential.

Including nuclei leads to a higher sensitivity due to a larger amount of baryons. A fit to the data in the most central collisions (0–5 % centrality) provides a value of μ_B that is close to zero. Using the antiparticle-to-particle ratios reduces the uncertainties by one order of magnitude with respect to the statistical hadronization model fit thanks to the direct cancellation of correlated uncertainties.

Figure 6 shows the antiparticle-to-particle ratios of pion, proton, hypertriton, and ^{3}He compared to the statistical hadronization model at $T_{\rm ch} = 155 \pm 2$ MeV and using the obtained μ_B. The vertical lines on the data points denote the statistical uncertainties. The lower panel shows the deviation from the model in number of standard deviations. The result is very precise even with large uncertainties for the hypertriton and a small overestimation for the ^{3}He.

5. Conclusion

Hypertriton results from the pp, p–Pb, and Pb–Pb data sets collected with the ALICE apparatus have been presented and compared with theoretical predictions. Due to its large size the hypertriton is the ideal candidate to distinguish between the different production models.

The $^3_\Lambda$H/Λ and S_3 ratios versus multiplicity clearly favour the coalescence over the statistical hadronization model. In the $^3_\Lambda$H/Λ case the statistical hadronization model implementation with

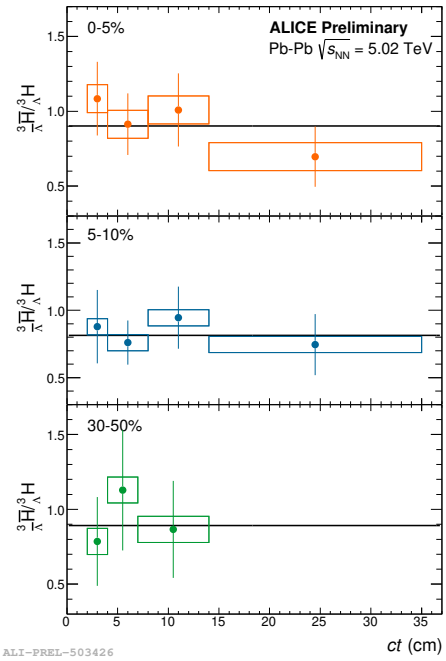

Figure 5. Antihypertriton-to-hypertriton ratio in Pb–Pb collisions at $\sqrt{s_{\rm NN}} = 5.02\,\text{TeV}$ measured in three centrality intervals.

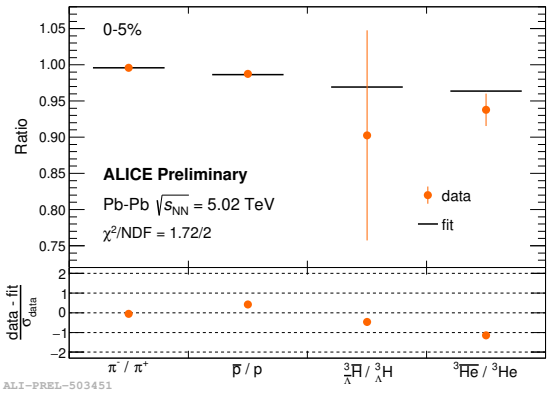

Figure 6. Antiparticle-to-particle ratios for pion, proton, hypertriton, and ^{3}He in Pb–Pb collisions at $\sqrt{s_{\rm NN}} = 5.02\,\text{TeV}$ compared with statistical hadronization model predictions.

the larger correlation volume is even ruled out by more than $6\,\sigma$.

The most precise measurements to date of the hypertiton lifetime and Λ separation energy have been obtained in Pb–Pb collisions at $\sqrt{s_{\rm NN}} = 5.02\,\text{TeV}$. The lifetime is compatible with the free Λ lifetime, which supports a very loosely-bound state. The Λ separation energy is compatible with the latest theoretical predictions.

The hypertriton and antihypertriton yields were measured in three centrality intervals in Pb–Pb collisions at $\sqrt{s_{\rm NN}} = 5.02\,\text{TeV}$. The baryochemical potential was determined using the antiparticle-to-particle ratios including the hypertriton. A value close to zero in central Pb–Pb collisions was obtained.

References

[1] Andronic A, Braun-Munzinger P, Stachel J and Stöcker H 2011 *Phys. Lett.* **B697** 203–207 (*Preprint* 1010.2995)
[2] Dönigus B 2020 *Int. J. Mod. Phys. E* **29** 2040001 (*Preprint* 2004.10544)
[3] Scheibl R and Heinz U 1999 *Physical Review C* **59** 1585–1602 ISSN 1089-490X
[4] Kapusta J I 1980 *Phys. Rev.* **C21** 1301–1310
[5] Sun K J, Ko C M and Dönigus B 2019 *Phys. Lett.* **B792** 132–137 (*Preprint* 1812.05175)
[6] Hildenbrand F and Hammer H W 2019 *Phys. Rev. C* **100** 034002 [Erratum: Phys.Rev.C 102, 039901 (2020)] (*Preprint* 1904.05818)
[7] ALICE Collaboration 2022 *Phys. Rev. Lett.* **128** 252003 (*Preprint* 2107.10627)
[8] Vovchenko V, Dönigus B and Stöcker H 2018 *Phys. Lett.* **B785** 171–174 (*Preprint* 1808.05245)
[9] ALICE Collaboration 2016 *Phys. Lett. B* **754** 360–372 (*Preprint* 1506.08453)
[10] ALICE Collaboration 2022 (*Preprint* 2209.07360)